Electronic Supplementary Material (ESI) for Nanoscale.


# Supporting Information

## Facile synthesis of Bismuth nanostructure with enhanced selectivity for electrochemical conversion of $CO_2$ to formate

Peilong Lu, et al.

*corresponding author: zhanggj@ipe.ac.cn (G. Zhang)

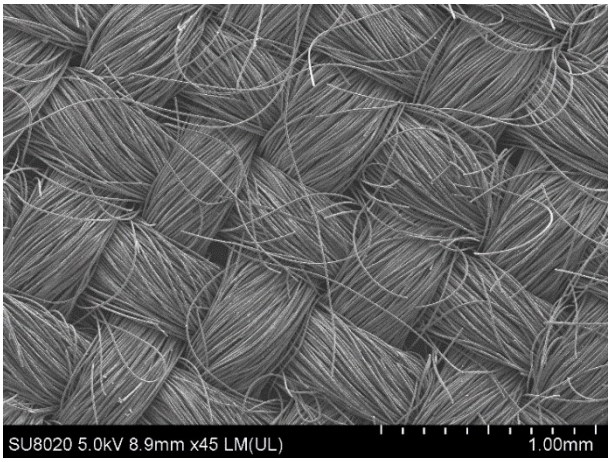


**Figure S1.** SEM image of hydrophilic carbon cloth.

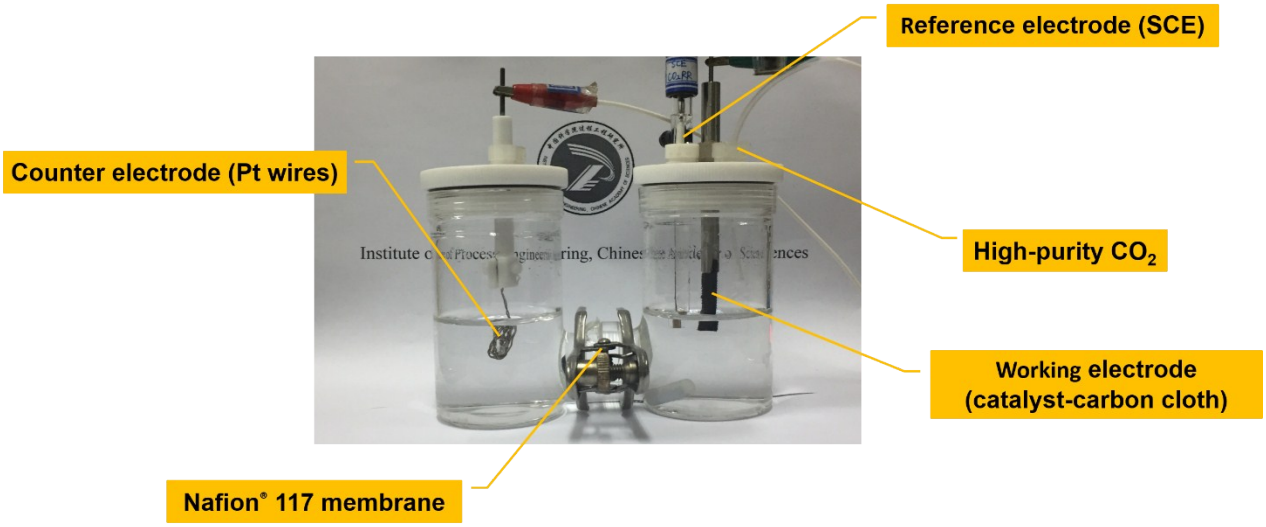


**Figure S2.** Digital photograph of the custom-made H-type electrolytic cell for $CO_2$ reduction reaction.

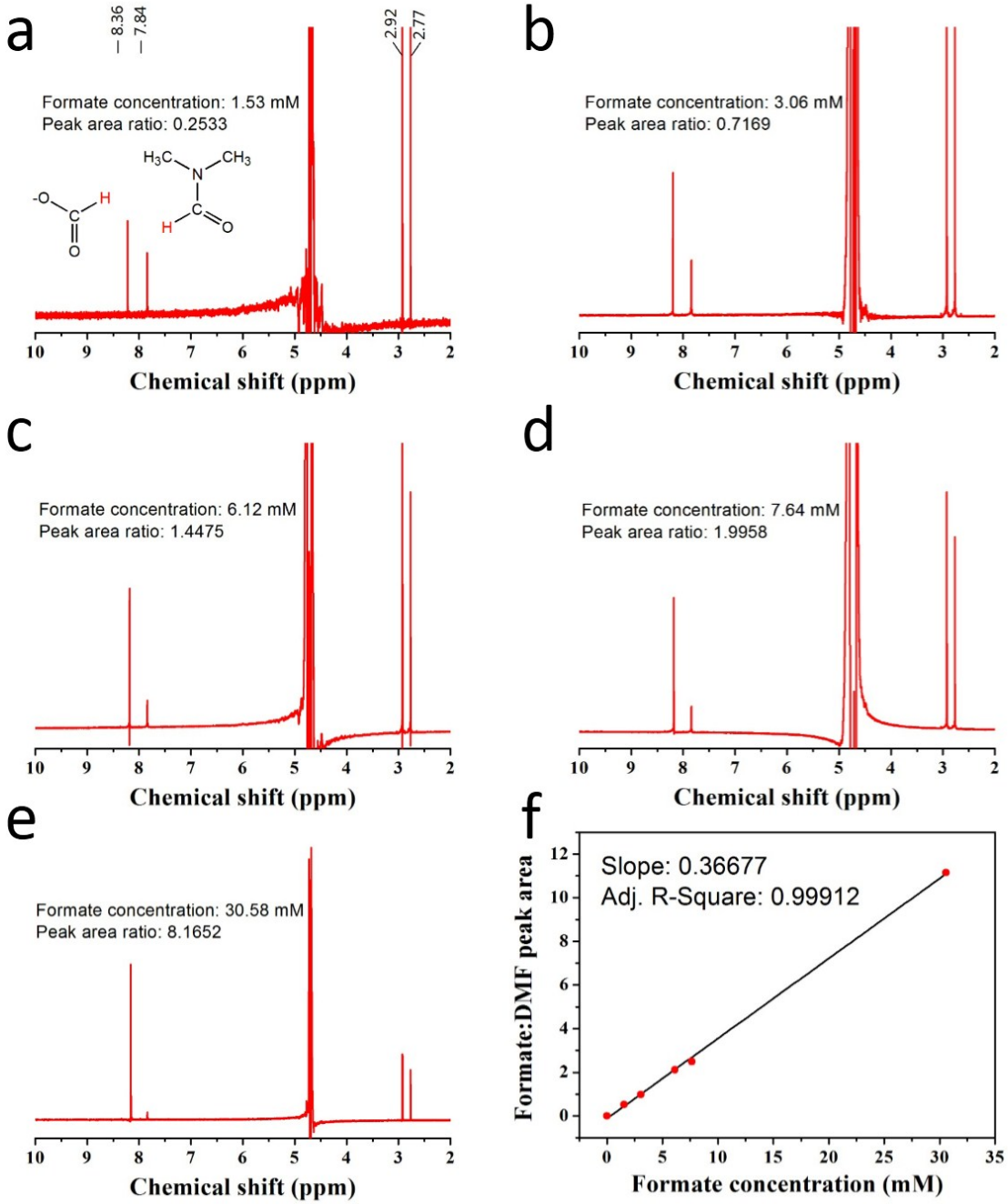


**Figure S3.** $^{1}$H NMR spectra of different formate acid concentrations: (a) 1.53 mM, (b) 3.06 mM, (c) 6.12 mM, (d) 7.64 mM, and (e) 30.58 mM. $c_{(DMF)}$: 12.90 mM. (f) The proportional relationship between formate concentration and relative peak area vs DMF. The linear correlation coefficient is 0.99912.

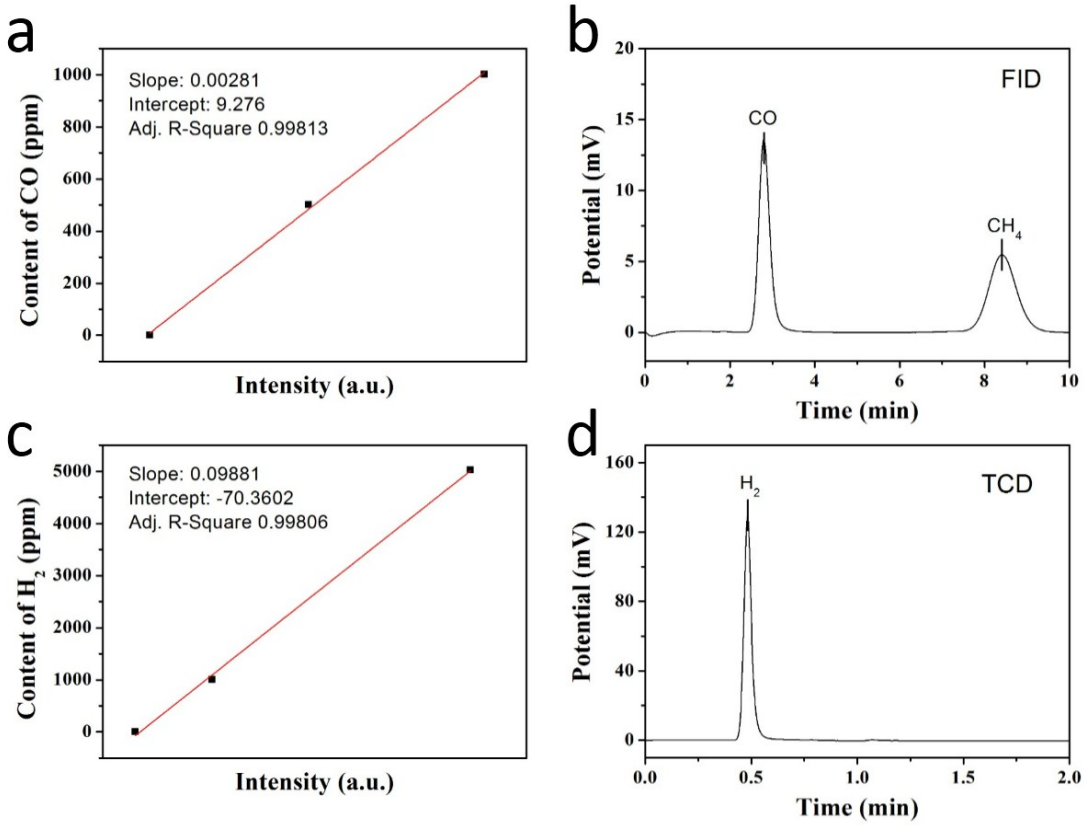


**Figure S4.** The calibration curves of (a) CO, (b) corresponding chromatographic peak, and (c) $H_2$, (d) corresponding chromatographic peak.

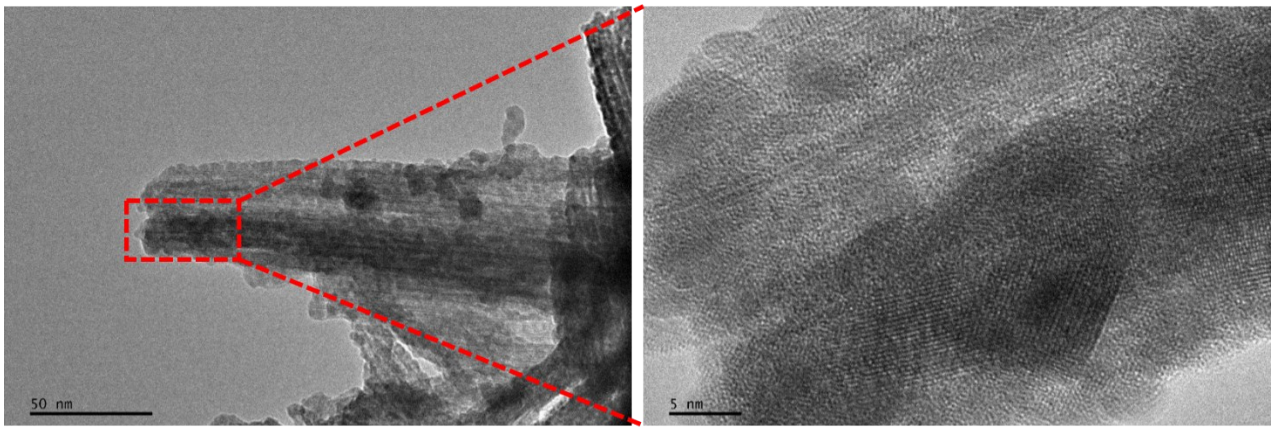


**Figure S5.** TEM images of bi nanostructure show its curved sheet structure.

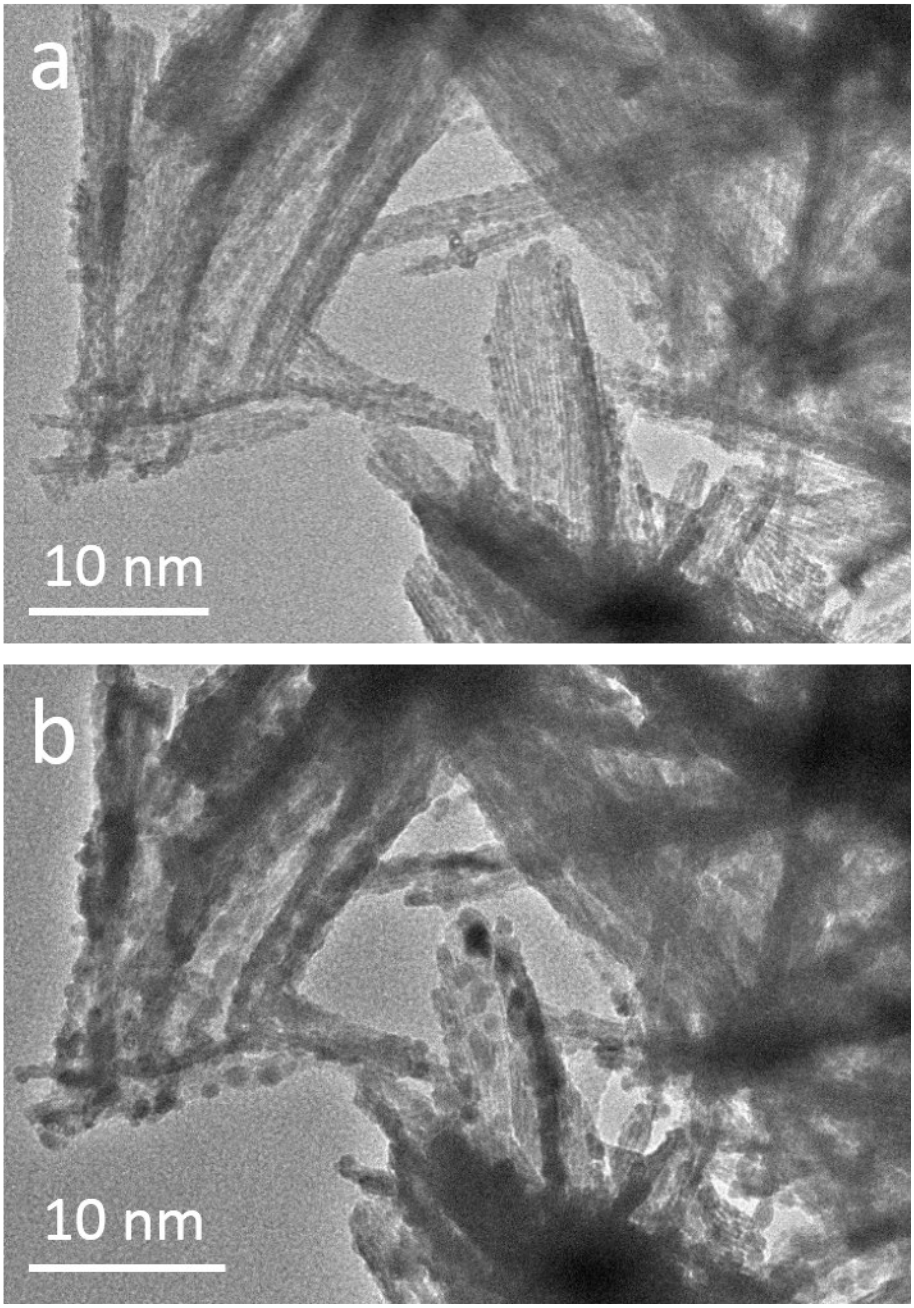


**Figure S6.** TEM image of (a) Bi nanostructure and (b) Bi nanostructure with certain length of time electron radiation, which the temperature will raise in this region.

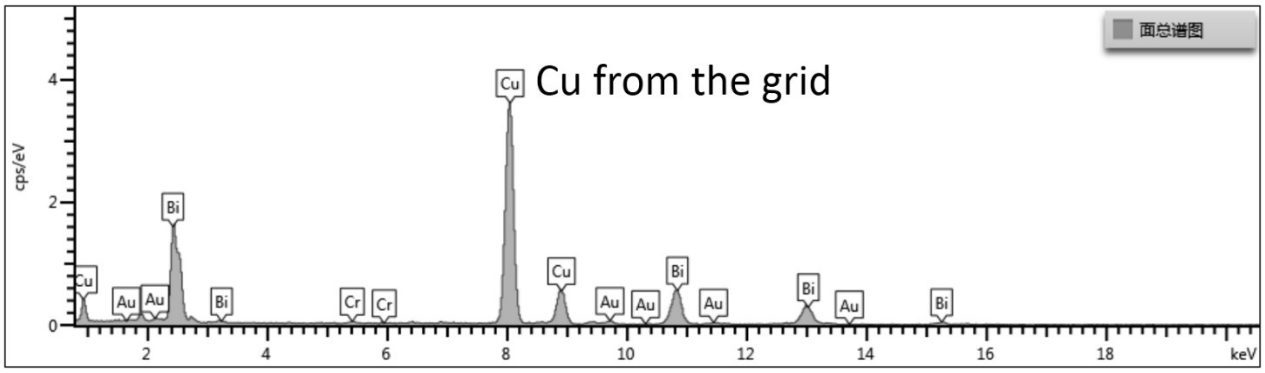


**Figure S7.** EDS spectrum of Bi nanostructure.

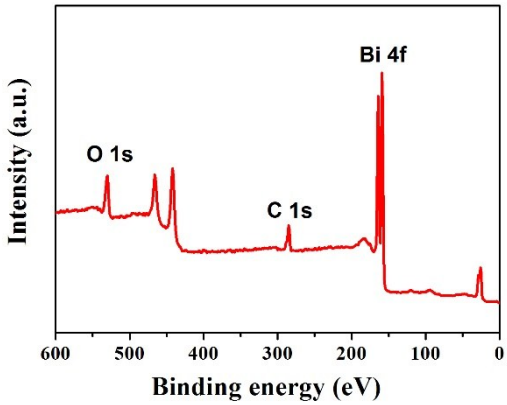


**Figure S8.** Full XPS survey of Bi nanostructure.

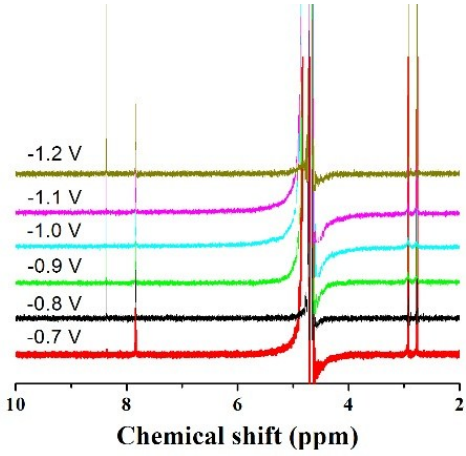


**Figure S9.** $^{1}$H NMR spectra of 1-hour-electrolysis electrolyte at given different potentials. Peaks at 8.36 ppm can be attributed to $HCOO^{-}$, while peaks at 7.84, 2.94 and 2.77 ppm can be assigned to DMF.

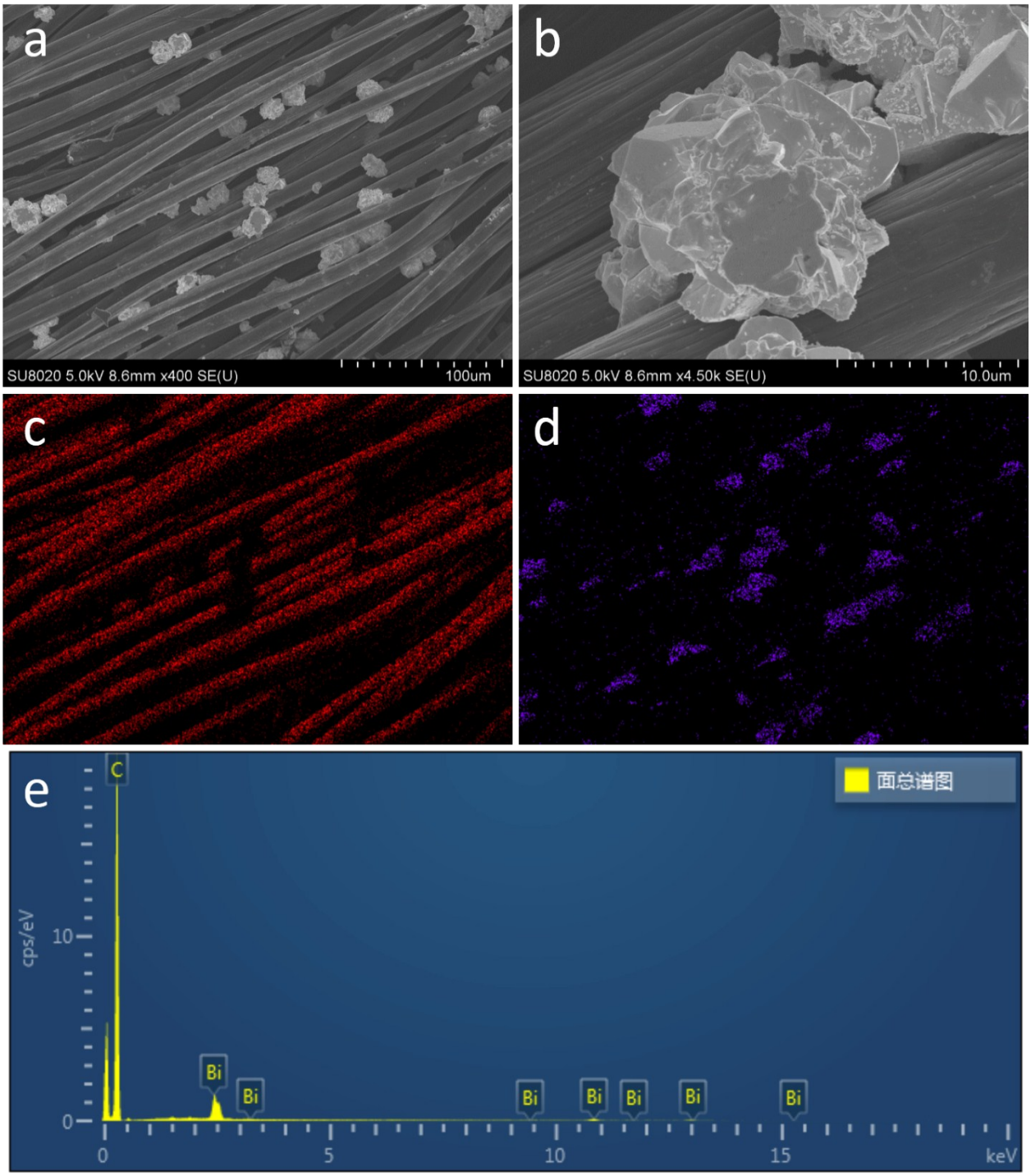


**Figure S10.** (a) SEM image of Bi deposit, (b) magnified Bi particle, corresponding EDS element mapping for (c) C and (d) Bi, and (e) EDS spectrum.

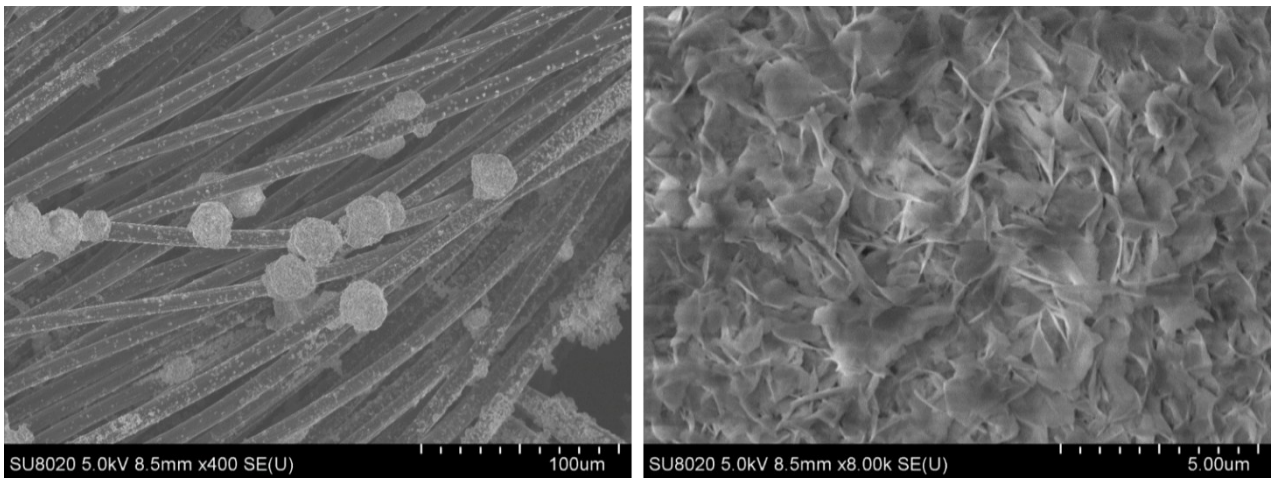


**Figure S11.** (a) SEM image of Bi deposit after electrolysis, and (b) magnified Bi particle.

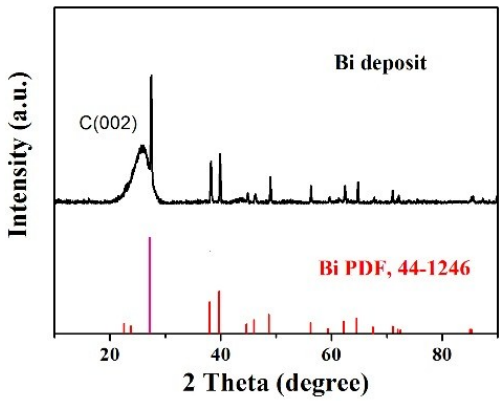


**Figure S12.** XRD pattern of Bi deposit. The intense and broad peak is from carbon cloth substrate.

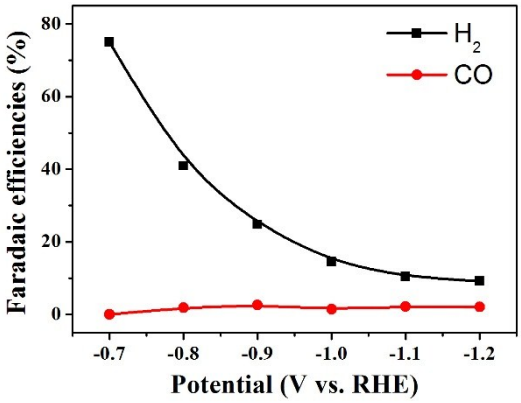


**Figure S13.** Faradaic efficiencies of $H_2$ and CO generated on Bi deposit electrode.

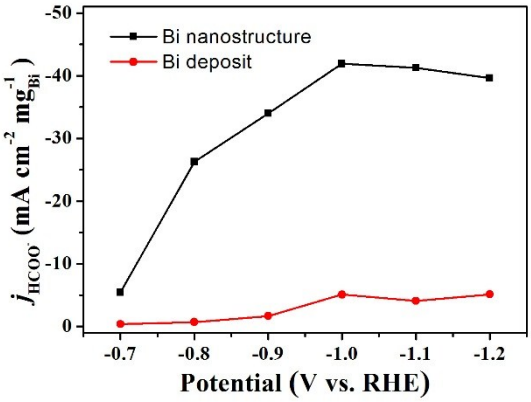


**Figure S14.** Mass-specific formate partial current density of Bi nanostructure and Bi deposit.

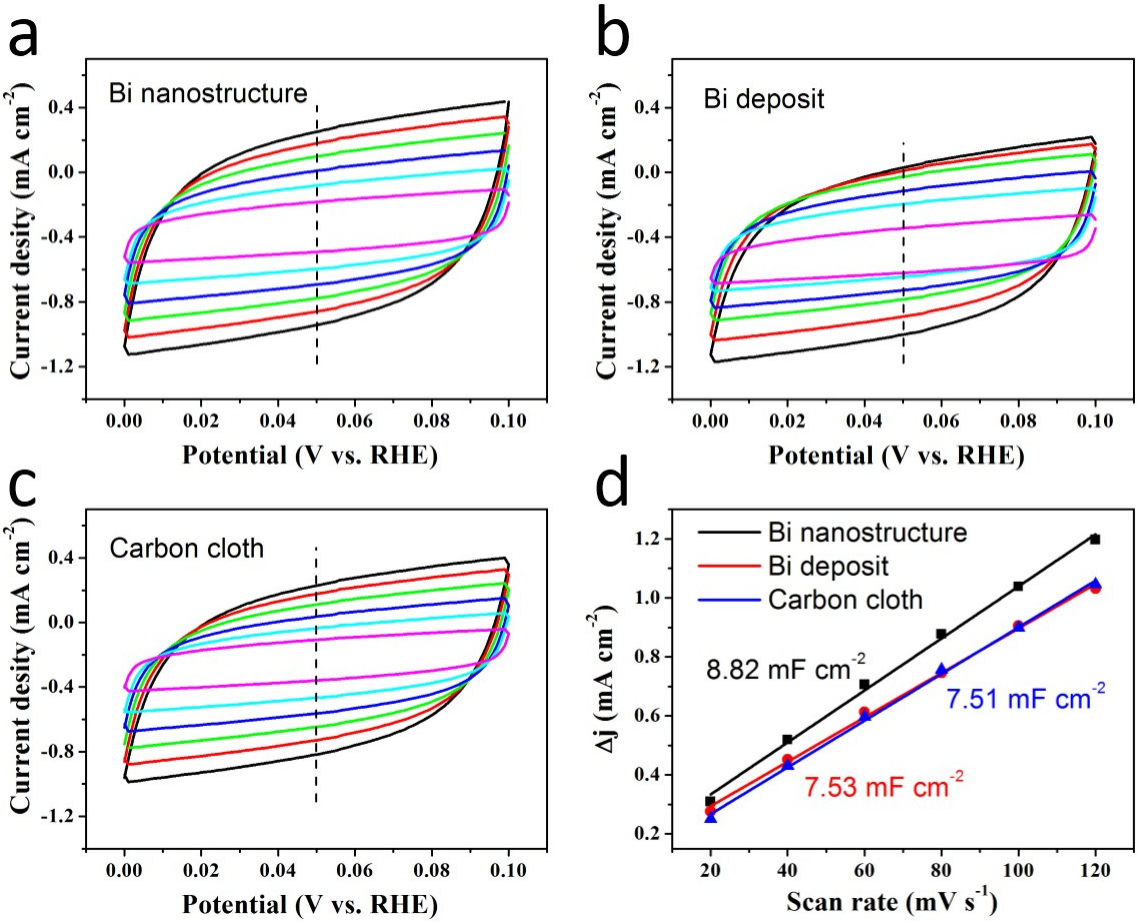


**Figure S15.** Cyclic voltammetry (CV) of (a) Bi nanostructure, (b) Bi deposit and (c) carbon cloth performed in $CO_2$-saturated 0.5 M $KHCO_3$ at various scan rates for measurement of double layer capacity. Cycle voltammetry was carried out between 0 and 0.1 V vs. RHE. Scan rates (mV $s^{-1}$) of 20 (pink), 40 (blue), 60 (mazarine), 80 (green), 100 (red) and 120 (black) were conducted. (d) The plots of double layer current versus CV scan rates.

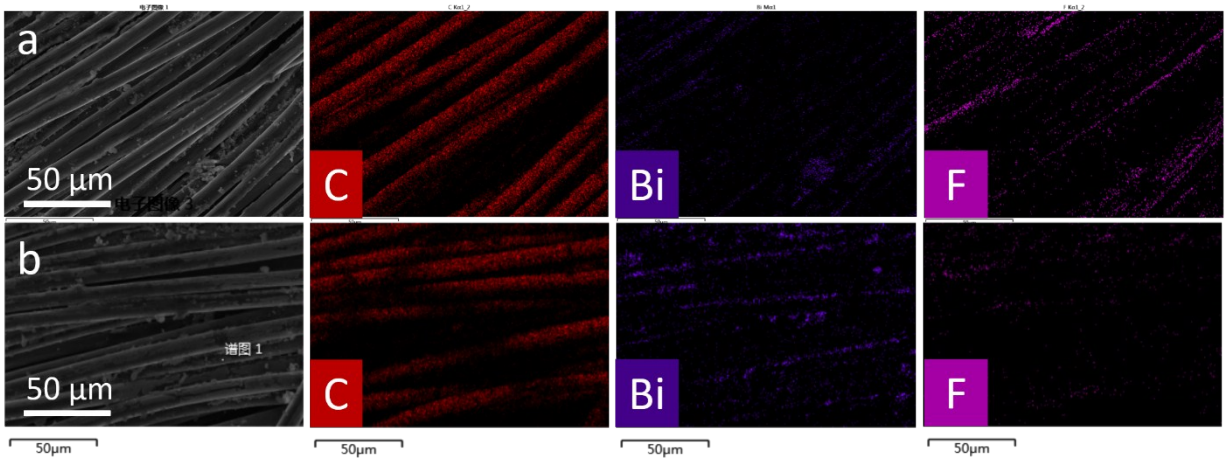


**Figure S16.** SEM images and corresponding EDS mapping of (a) Bi nanostructure loading on Carbon cloth (a) before and (b) after the stability test. The element of F comes from Nafion 117.

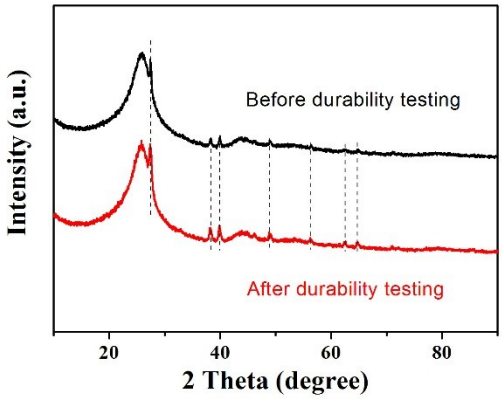


**Figure S17.** XRD patterns of Bi nanostructure (loading on Carbon cloth) before (black) and after (red) the stability test.

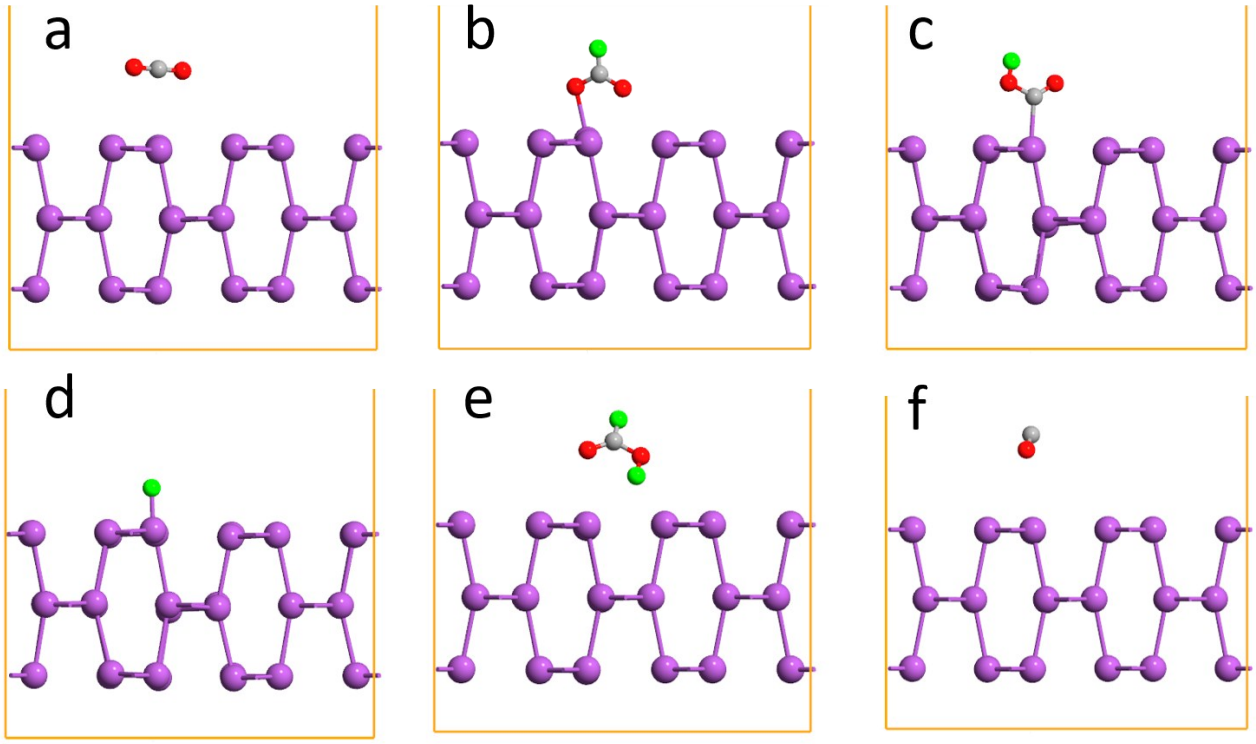


**Figure S18.** DFT simulation optimized geometric structure of (a) $CO_2$, (b) *OCHO adsorbate, (c) *COOH adsorbate, (d) *H adsorbate, (e) formate and (f) CO, where Bi, C, O, and H atom were presented by purple, grey, red and green spheres, respectively.

**Table S1.** Selected Calculated standard reduction potential values in acid (V vs. RHE) for various $CO_2RR$ products, in comparison with hydrogen evolution reaction (HER).[1]

| Product | Equation | E (V) |
|---|---|---|
| Hydrogen | $2H^+ + 2e^- \rightarrow \mathbf{H_2}$ | E = 0 V |
| Carbon monoxide | $CO_2 + 2H^+ + 2e^- \rightarrow \mathbf{CO} + H_2O$ | E = -0.104 V |
| Formic acid/formate | $CO_2 + 2H^+ + 2e^- \rightarrow \mathbf{HCOOH}$ | E = -0.171 V |
| Formaldehyde | $CO_2 + 4H^+ + 4e^- \rightarrow \mathbf{HCHO} + H_2O$ | E = -0.142V |
| Methanol | $CO_2 + 6H^+ + 6e^- \rightarrow \mathbf{CH_3OH} + H_2O$ | E = 0.016 V |
| Glyoxal | $2CO_2 + 6H^+ + 6e^- \rightarrow \mathbf{CHOCHO} + 2H_2O$ | E = -0.141 V |
| Methane | $CO_2 + 8H^+ + 8e^- \rightarrow \mathbf{CH_4} + 2H_2O$ | E = 0.169 V |
| Acetic acid/acetate | $2CO_2 + 8H^+ + 8e^- \rightarrow \mathbf{CH_3COOH} + 2H_2O$ | E = 0.098 V |
| Acetaldehyde | $2CO_2 + 10H^+ + 10e^- \rightarrow \mathbf{CH_3CHO} + 3H_2O$ | E = 0.053 V |
| Ethane | $CO_2 + 12H^+ + 12e^- \rightarrow \mathbf{C_2H_4} + 4H_2O$ | E = 0.085 V |
| Ethanol | $CO_2 + 12H^+ + 12e^- \rightarrow \mathbf{C_2H_5OH} + 3H_2O$ | E = 0.084 V |

**Table S2.** Selected reported formate-acid-producing electrocatalysts for $CO_2RR$.

| Reference | Catalyst | FE | Potential vs. RHE(V) | Current density (mA $cm^{-2}$) | Loading (mg $cm^{-2}$) | Medium |
|---|---|---|---|---|---|---|
| **1 This work** | **Bi** | **92%** | **-0.9** | **-15** | **0.4** | **0.5 M $KHCO_3$** |
| **2** [2] | Few-layer-Bi | 85% | -0.8 | -10.48 | ~1 | 0.5 M $NaHCO_3$ |
| **3** [3] | $Bi_2S_3$-derived Bi | 84% | -0.75 | -5 | 0.34 | 0.5 M $NaHCO_3$ |
| **4** [4] | $Bi_{45}$ | 90% | -0.78 | -1.5 | 3 | 0.5M $KHCO_3$ |
| **5** [5] | Bi nanodendrites | 96.4% | -1.13 | -15.2 | N/A | 0.5 M $NaHCO_3$ |
| **6** [6] | Bi/CF | 78% | -0.73 | -53 | N/A | 0.1 M $KHCO_3$ |
| **7** [7] | Utrathin Bi nanosheets | ~100% | -0.9 | -15 | 1 | 0.5 M $KHCO_3$ |
| **8** [6] | Bi-Sn | 96% | -1.14 | -45 | N/A | 0.5 M $KHCO_3$ |
| **9** [8] | $Ag_3Sn$ | 87% | -0.9 | -20 | 1 | 0.5 M $NaHCO_3$ |
| **10** [9] | $CuSn_3$ | 95% | -0.5 | -31 | N/A | 0.1 M $KHCO_3$ |
| **11** [10] | Pb/Cu | 81.4±5.2 % | -1.17 | N/A | N/A | 0.1 M $KHCO_3$ |
| **12** [11] | Pd nanosheets | 89% | -0.57 | ≈ -13 | N/A | 0.1 M $NaHCO_3$ |
| **13** [12] | S-modulated Tin sites | 93% | -0.75 | -55 | N/A | 0.1 M $KHCO_3$ |
| **14** [13] | Sn quantum sheets | 93% | -1.1 | -25 | N/A | 0.1 M $NaHCO_3$ |
| **15** [14] | SnO*x*/Graphene | 94% | -1.16 | -10 | 0.21 | 0.1 M $NaHCO_3$ |
| **16** [15] | Sn/SnO*x* thin film | 40% | -0.7 | -4 | N/A | 0.5 M $NaHCO_3$ |
| **17** [16] | Electroplated | 71% | -1.10 | -20 | N/A | 0.5 M $NaHCO_3$ |
| **18** [17] | Sn modified N-doped carbon nanofiber | 62% | -0.8 | -9 | N/A | 0.5 M $KHCO_3$ |
| **19** [18] | SnO nanoparticles | 75% | -0.86 | -10 | 0.3 | 0.5 M $KHCO_3$ |

**References**


1. A. D. Handoko, F. Wei, Jenndy, B. S. Yeo and Z. W. Seh, *Nat. Catal.*, 2018, **1**, 922-934.
2. Y. Zhang, X. Zhang, Y. Ling, F. Li, A. M. Bond and J. Zhang, *Angew. Chem. Int. Ed.*, 2018, **57**, 13283-13287.
3. Y. Zhang, F. Li, X. Zhang, T. Williams, C. D. Easton, A. M. Bond and J. Zhang, *J. Mater. Chem. A*, 2018, **6**, 4714-4720.
4. X. Zhang, T. Lei, Y. Liu and J. Qiao, *Appl. Catal. B: Environ.*, 2017, **218**, 46-50.
5. H. Zhong, Y. Qiu, T. Zhang, X. Li, H. Zhang and X. Chen, *J. Mater. Chem. A*, 2016, **4**, 13746-13753.
6. G. Wen, D. U. Lee, B. Ren, F. M. Hassan, G. Jiang, Z. P. Cano, J. Gostick, E. Croiset, Z. Bai, L. Yang and Z. Chen, *Adv Energy Mater*, 2018, **8**, 1802427.
7. N. Han, Y. Wang, H. Yang, J. Deng, J. Wu, Y. Li and Y. Li, *Nat Commun*, 2018, **9**, 1320.
8. W. Luc, C. Collins, S. Wang, H. Xin, K. He, Y. Kang and F. Jiao, *J Am Chem Soc*, 2017, **139**, 1885-1893.
9. X. Zheng, Y. Ji, J. Tang, J. Wang, B. Liu, H.-G. Steinrück, K. Lim, Y. Li, M. F. Toney, K. Chan and Y. Cui, *Nat. Catal.*, 2019, **2**, 55-61.
10. C. Kim, T. Möller, J. Schmidt, A. Thomas and P. Strasser, *ACS Catal.*, 2018, 1482-1488.
11. J. Xie, X. Wang, J. Lv, Y. Huang, M. Wu, Y. Wang and J. Yao, *Angew Chem Int Ed Engl*, 2018, **57**, 16996-17001.
12. X. Zheng, P. De Luna, F. P. García de Arquer, B. Zhang, N. Becknell, M. B. Ross, Y. Li, M. N. Banis, Y. Li, M. Liu, O. Voznyy, C. T. Dinh, T. Zhuang, P. Stadler, Y. Cui, X. Du, P. Yang and E. H. Sargent, *Joule*, 2017, **1**, 794-805.
13. F. Lei, W. Liu, Y. Sun, J. Xu, K. Liu, L. Liang, T. Yao, B. Pan, S. Wei and Y. Xie, *Nat. Commun.*, 2016, **7**, 12697.
14. S. Zhang, P. Kang and T. J. Meyer, *J. Am. Chem. Soc.*, 2014, **136**, 1734-1737.
15. Y. Chen and M. W. Kanan, *J. Am. Chem. Soc.*, 2012, **134**, 1986-1989.
16. E. Irtem, T. Andreu, A. Parra, M. D. Hernández-Alonso, S. García-Rodríguez, J. M. Riesco-García, G. Penelas-Pérez and J. R. Morante, *J. Mater. Chem. A*, 2016, **4**, 13582-13588.
17. Y. Zhao, J. Liang, C. Wang, J. Ma and G. G. Wallace, *Adv Energy Mater*, 2018, **8**, 1702524.
18. J. Gu, F. Héroguel, J. Luterbacher and X. Hu, *Angew. Chem.*, 2018, **130**, 2993-2997.